

## Article

# Self-Healing, Flexible and Smart 3D Hydrogel Electrolytes Based on Alginate/PEDOT:PSS for Supercapacitor Applications

Nujud M. Badawi <sup>1</sup>, Mamta Bhatia <sup>2</sup>, S. Ramesh <sup>1</sup>, K. Ramesh <sup>1,\*</sup>, Mufsir Kuniyil <sup>3</sup>,  
Mohammed Rafi Shaik <sup>3</sup>, Mujeeb Khan <sup>3</sup>, Baji Shaik <sup>4</sup> and Syed F. Adil <sup>3,\*</sup>

<sup>1</sup> Centre for Ionics, Department of Physics, Faculty of Science, Universiti Malaya, Kuala Lumpur 50603, Malaysia

<sup>2</sup> Department of Physics, Acharya Narendra Dev College, University of Delhi, Delhi 110019, India

<sup>3</sup> Department of Chemistry, College of Science, King Saud University, P.O. Box 2455, Riyadh 11451, Saudi Arabia

<sup>4</sup> School of Chemical Engineering, Yeungnam University, Gyeongsan 38541, Republic of Korea

\* Correspondence: rameshkasi@um.edu.my (K.R.); sfadil@ksu.edu.sa (S.F.A.)

**Abstract:** Hydrogel electrolytes for energy storage devices have made great progress, yet they present a major challenge in the assembly of flexible supercapacitors with high ionic conductivity and self-healing properties. Herein, a smart self-healing hydrogel electrolyte based on alginate/poly(3,4-ethylenedioxythiophene):poly(styrenesulfonate) (alginate/PEDOT:PSS)(A/P:P) was prepared, wherein H<sub>2</sub>SO<sub>4</sub> was employed as a polymeric initiator, as well as a source of ions. PEDOT:PSS is a semi-interpenetrating network (IPN) that has been used in recent studies to exhibit quick self-healing properties with the H<sub>2</sub>SO<sub>3</sub> additive, which further improves its mechanical strength and self-healing performance. A moderate amount of PEDOT:PSS in the hydrogel (5 mL) was found to significantly improve the ionic conductivity compared to the pure hydrogel of alginate. Interestingly, the alginate/PEDOT:PSS composite hydrogel exhibited an excellent ability to self-heal and repair its original composition within 10 min of cutting. Furthermore, the graphite conductive substrate-based supercapacitor with the alginate/PEDOT:PSS hydrogel electrolyte provided a high specific capacitance of 356 F g<sup>-1</sup> at 100 mV/s g<sup>-1</sup>. The results demonstrate that the A/P:P ratio with 5 mL PEDOT:PSS had a base sheet resistance of 0.9 Ω/square. This work provides a new strategy for designing flexible self-healing hydrogels for application in smart wearable electronics.

**Keywords:** flexible; self healing; smart hydrogel; electrolyte; supercapacitor



**Citation:** Badawi, N.M.; Bhatia, M.; Ramesh, S.; Ramesh, K.; Kuniyil, M.; Shaik, M.R.; Khan, M.; Shaik, B.; Adil, S.F. Self-Healing, Flexible and Smart 3D Hydrogel Electrolytes Based on Alginate/PEDOT:PSS for Supercapacitor Applications.

*Polymers* **2023**, *15*, 571. <https://doi.org/10.3390/polym15030571>

Academic Editor: Yiwan Huang

Received: 22 December 2022

Revised: 18 January 2023

Accepted: 18 January 2023

Published: 22 January 2023



**Copyright:** © 2023 by the authors. Licensee MDPI, Basel, Switzerland. This article is an open access article distributed under the terms and conditions of the Creative Commons Attribution (CC BY) license (<https://creativecommons.org/licenses/by/4.0/>).

## 1. Introduction

With the recent development of smart wearable electronics, such as portable biosensors, watches, and smart textiles, it is imperative that energy storage systems be reliable in the face of mechanical damage [1,2]. Recently, self-healing flexible supercapacitors have received increasing attention, because smart electrochemical capacitors (ECs) have high specific capacitance, energy and power densities, cycle life, and fast charge–discharge processes [3–6]. In addition, flexible hydrogel electrolytes play an essential role in the discharging and charging of supercapacitors. Self-healing polymers are often used for the synthesis of electrolytes, where good electrochemical properties are very important in supercapacitors [7]. In recent decades, supercapacitors and various types of electrolytes, including gels, aqueous, and ionic liquids with redox activity, that are suitable for large-scale manufacturing have been designed and tested. Conversely, energy storage devices that use liquid electrolytes or those based on solid polymer electrolytes require a high standard of materials for safe encapsulation, with variable geometries. This opens new opportunities for the development of energy storage devices in the field of smart wearable electronics [8]. Simultaneously, it is important for smart electrochemical capacitors to possess the self-healing properties of the hydrogel electrolyte, because it directly restores

its capacitive performance when subjected to misuse, such as cutting or breakage, in record time [9–11].

To introduce the features of self healing and flexibility into high-performance hydrogel solutions, alginate is used as a polymeric substrate, which not only induces super-elasticity in the electrolyte, but also acts as a stable and environmentally friendly precursor [12–14]. There have been several reports on the use of polymeric alginate along with acidic KCl,  $H_3BO_3$ , KOH, and LiCl [15–17]. However, the use of inorganic ions to maintain the conductive nature of the polymer while inducing flexibility exerts an unfavorable effect owing to the interference of the ions within the polymeric framework. The ions adversely affect the intracellular hydrogen bonds between the conductive and flexible components of the composite polymer, resulting in poor self healing [15,18]. To deal with this problem, the polymer electrolytes must initially be solid. Furthermore, these electrolytes are to be treated with inorganic ions to be strong enough to support the massive deformation caused by the non-covalent hydrogen bonding [19] and coordination [20] bonds, thus forming flexible conductive polymer electrolytes with high curability.

The incorporation of physical (conformational alterations) and chemical (bond formation) mechanisms enhances the self-healing capabilities of maintenance-free materials [21]. Therefore, the dynamics of the interplay of movable crosslinks and reversible bonds has prompted the proposal of a composite hydrogel electrolyte, leading to its sustainable application in wearable electronics with fast self-healing properties [22].

Currently, composite polymers such as PEDOT:PSS (a good example of semi IPN) have attracted a great deal of attention, as they are used in various electrochemical devices such as fuel cells [23], dye-sensitive solar cells, and supercapacitors [24] due to their high ionic conductivity property [25–27]. Moreover, their flexibility and self-healing properties have been studied with the application of polyethylene glycol and alginate, and their effects on the tensile strength of the resulting conductive polymer have been reported. In addition, a study by Meen et al. [23] reported that the addition of dilute  $H_2SO_4$  boosted the conductivity of the composite (PEDOT:PSS) by significantly reducing the sheet resistance. This reduction in sheet resistance was attributed to the fact that nonconductive anions of some  $PSS^-$  were replaced by conductive anions of  $H_2SO_4$ . They reported that this substitution reaction caused greater aggregation of PEDOT chains, favoring the enhancement of conductivity and leading to high transmittance and transparency. Their work thus indicated that  $H_2SO_4$  doping in PEDOT:PSS films can prove useful in optoelectronic devices, in which transparent conductive electrodes find application [24].

Similarly, Shi et al. reported a wet process for the fabrication of electrochemical capacitors (ECs) using acid-treated ( $H_2SO_4$ ) PEDOT:PSS as an electrode material and graphite foil as the current collector. The as-fabricated EC exhibited excellent electrochemical stability with high areal ( $994 \mu F cm^{-2}$ ) and volumetric ( $16.6 F cm^{-3}$ ) specific capacitances at 120 Hz [28]. The same group also reported a PEDOT:PSS-based ultrahigh-conductive polymer hydrogel that was prepared by the thermal treatment of PEDOT:PSS with  $H_2SO_4$  [28]. The polymer-based hydrogel supercapacitor demonstrated high volumetric capacitance ( $202 F cm^{-3}$  at  $0.54 A cm^{-3}$ ), with an extraordinarily high level of performance, which can be easily fabricated in diverse forms, including as films, fibers and columns. Additionally, PEDOT:PSS-based functional tough hydrogels have also been used in various other advanced devices for translational applications [29].

In this work, we report the preparation of an alginate/PEDOT:PSS hydrogel, wherein  $H_2SO_4$  is employed for dual purposes—as both the polymerization initiator and the source of ions within the polymeric framework—with the aim of improving ionic conductivity, hydrogen bonding, and coordination. Thus, the use of  $H_2SO_4$  led to the formation of flexible conductive polymer electrolytes with high curability. Based on the properties of conducting polymers such as PEDOT:PSS, Song et al. [30] reported their application as semitransparent supercapacitors with high conductivity via  $H_2SO_3$  treatment. Hina et al. [31] reported the fabrication of aqueous solid-state supercapacitors based on poly(PEDOT:PSS) composite hydrogel electrolytes through free-radical polymerization. For this fabrication, they added

sodium montmorillonite clay as a crosslinker. The present work demonstrates the novelty of the rapid self-healing properties of alginate/PEDOT:PSS with the addition of  $\text{H}_2\text{SO}_3$ . Notably, in comparison with pure hydrogel alginate, the addition of PEDOT:PSS enhanced the ionic conductivity to a great extent, and also showed rapid self healing within minutes of cutting.

## 2. Results and Discussion

### 2.1. Synthesis of Composite Hydrogel Electrolytes

An alginate/PEDOT:PSS hydrogel electrolyte was prepared using  $\text{H}_2\text{SO}_4$  as an initiator of alginate polymerization while encapsulating the PEDOT:PSS in the framework. This yielded an electrically conductive hydrogel made up of alginate gel with PEDOT:PSS trapped in the framework (Figure 1).

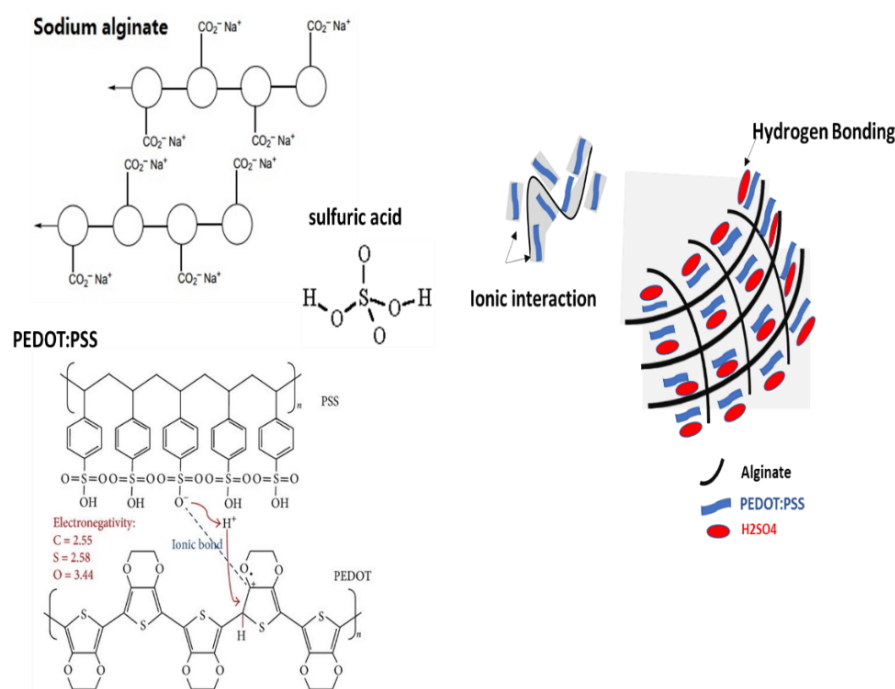


**Figure 1.** Schematic illustration of mixed ionic and electronic conduction in composite hydrogel electrolyte.

### 2.2. Physical Crosslinked Alginate/PEDOT:PSS Hydrogel

Strong interactions between chains is a distinctive feature of alginate/PEDOT:PSS hydrogels, because a stable linkage forms in the molecular network. The alginate polymer network makes the entry and retention of water in the hydrogel easier. Through non-covalent methods such as hydrogen bonding and hydrophobic forces between polymer chains, hydrogels have been created. These reactions create hydrogels, which are physically only gels with a high degree of water sensitivity. Because hydrogels do not need any harmful chaperone particles, they are safe for use in flexible wearable technology [32]. Additionally, the hydrogel contains alginate, a type of normal anionic polysaccharide. The addition of  $\text{H}_2\text{SO}_4$  caused the hydrogel to crystallize, which caused the chains to be joined together by hydrogen bonding. Thus, the mechanical strength of the hydrogel increased compared to before crystallization. PEDOT:PSS affects the hydrogel characteristics. Moreover, the mechanical strength of the PEDOT:PSS hydrogel is improved by the addition of polysaccharides and alginate (Figure 1).

### 2.3. Morphology and Distribution of the Alginate/PEDOT:PSS Hydrogel Electrolyte

The microstructures of the alginate hydrogel and polymerized A/P:P hydrogel were studied using SEM. In the low-resolution images (Figure 2a,b), the three-dimensional mor-

phology appears to be flaky, with visible interconnection bridges. High-resolution images (Figure 2a,b) depict spherical pores on the flake-like hydrogel surface [33]. According to the SEM images of all the samples in Figure 2, the pore diameters of the hydrogels before adding PEDOT:PSS were larger compared to A/P:P. This is because of the viscosity of PEDOT:PSS dispersion, which clogs the pores, thus reducing the pore size [33]. The displayed SEM images of hydrogels obtained by treatment with the hydrogel show a characteristic 3D fibrous network (Figure 2d–f). The alginate hydrogel surrounds PSS particles, and an organic network forms because of self-assembly in  $H_2SO_4$ . The nearby micelles physically intertwine via  $\pi$ - $\pi$  stacking and H bonding of PEDOT:PSS molecules [34], as well as through polar solvents such as water.

The PEDOT:PSS molecules form micellar structures. However, the surface morphology of the alginate hydrogel changed to a foam-like microstructure (Figure 2c,d) upon polymerization catalyzed by  $H_2SO_4$  in the presence of PEDOT:PSS [35].  $H_2SO_4$  catalyzes the inter-connection of the structure by forming cross-links and biphasic encapsulation of PEDOT:PSS at the hydrogel interface (Figure 2e,f) [36–38].

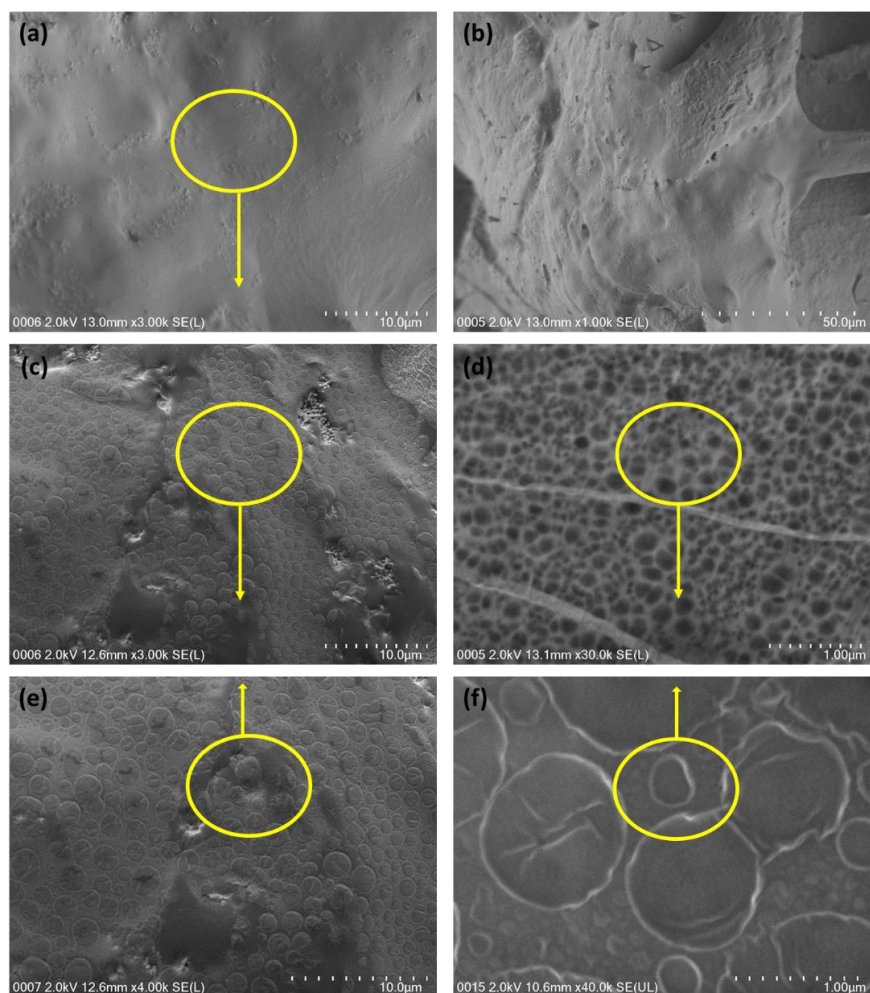


**Figure 2.** (a,b) SEM images of the alginate hydrogel and (c,d) the alginate/PEDOT:PSS hydrogel electrolyte at (e) low and (f) high magnification.

#### 2.4. FT-IR Spectra

The chemical structure of the ‘as-synthesized’ alginate/PEDOT:PSS hydrogel electrolyte was analyzed by FT-IR spectroscopy (Figure 3). The key to flexible curable conductive hydrogels is the use of a PEDOT:PSS synthetic polymer doped in an alginate solution and its subsequent conversion into a conductive hydrogel by polymerization with the addition of  $H_2SO_4$  under basic conditions [39]. The addition of PEDOT:PSS improved the

coagulation of organic hydrogel solution chains through ionic salt formation. The broad peak at  $3450\text{ cm}^{-1}$  for alginate and the alginate/PEDOT:PSS hydrogel is because of the partially overlapping stretching vibrations of the OH groups at high concentrations of PEDOT:PSS (5 mL) and NH groups in the gel state (Figure 3c). The peaks at  $2606$  and  $2400\text{ cm}^{-1}$  are due to the stretching vibrations of saturated C-H bonds, and the peaks at  $1623$  and  $1420\text{ cm}^{-1}$  correspond to the vibration of symmetric and asymmetric stretchings, respectively, of the bonds of  $\text{-COO-}$  groups in alginate [40]. The peak around  $1700\text{ cm}^{-1}$  is due to C=O. The peak at  $1060\text{ cm}^{-1}$  is caused by the stretching vibrations of the C-O-C groups, and the peak at  $1010\text{ cm}^{-1}$  is due to the  $\text{-O-C-O-}$  stretching vibrations of alginate. Some peaks disappeared in the FTIR spectrum of the PEDOT:PSS composite with respect to the alginate hydrogel spectrum [41]. The peak at  $1620\text{ cm}^{-1}$  for alginate/PEDOT:PSS is attributed to the expansion of vibrations of  $\text{-C=N}$  groups, which are produced through the chemical reaction of  $\text{-OH}$  in oxidized starch and  $\text{H}_2\text{N}^+$  in starch from wheat. In addition, the peak at  $1326\text{ cm}^{-1}$  is attributed to alginate with bending oscillations  $\text{-CH}_2\text{-SO}_3$  or  $\text{-N-CO-CH}_2\text{-}$  groups, which are from alginate/PEDOT:PSS [33–39,42].

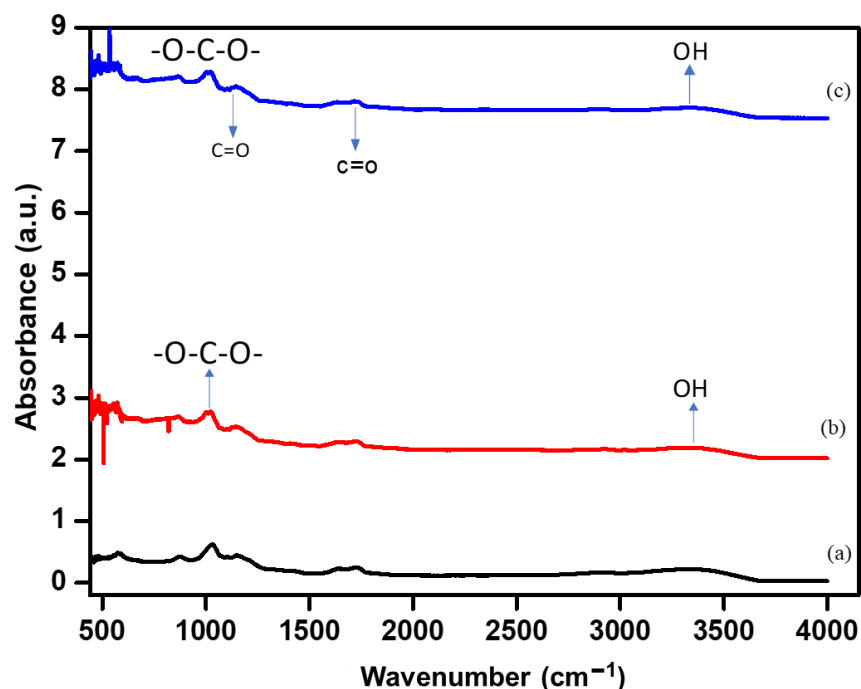


Figure 3. The FT-IR spectrum of the (a) alginate and (b,c) A/P:P hydrogel.

### 2.5. X-ray Diffraction Analysis (XRD)

The XRD patterns of all porous A/P:P were compared with that of the alginate hydrogel (control) sample, as shown in Figure 4. The presence of PEDOT:PSS in the alginate hydrogel can be clearly observed at A/P:P ratios of  $12.85^\circ$ ,  $15.65^\circ$ ,  $21.50^\circ$ , and  $32.50^\circ$ ; their corresponding Miller indices are (110), (210), (211), (310), and (121), respectively. These three major peaks are known as amorphous corona diffraction of PSS and interlaced packing of PEDOT [43]. All hydrogels are amorphous, but exhibit wide halos in their diffraction patterns, and the difference in the concentration ratio of PEDOT:PSS characterizes components with diffraction features located in different places and at different angles of scattering. The samples treated with PEDOT:PSS at a concentration of 5 mL appear in the form of triangles. Moreover, the peaks decrease in intensity in the hydrogel sample, and the increase in PEDOT:PSS in the pure hydrogel corresponds to the increase in its peak.

The shift of the peaks may be due to the conjugation of the hydrogel with PEDOT:PSS. The samples did not show any large crystalline peaks, owing to the amorphous structures of the alginate hydrogel [44]. The low intensity of PEDOT:PSS (2.5 and 5 mL) indicates

a decrease in the degree of crystallization because of the incorporation and interactions between the alginate hydrogel and PEDOT:PSS [45].

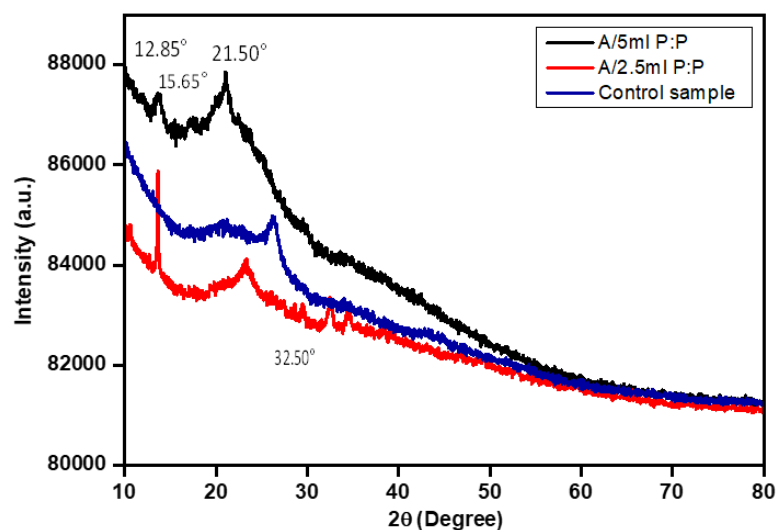


**Figure 4.** Relative intensity XRD plot of the alginate and A/P:P hydrogel.

#### 2.6. Electrochemical Studies of Alginate/PEDOT:PSS Hydrogel Conductive Coaxial and Galvanostatic Charge Discharge (GCD)

To further evaluate the applicability of the hydrogel electrolyte composites for supercapacitors, their specific capacitances, spin performances, and electrochemical stabilities were analyzed. A synthesized hydrogel electrolyte was inserted between the electrodes, and cyclic voltammetry (CV) was performed. The CV curves obtained by the alginate/PEDOT:PSS hydrogel electrolytes (by scanning at various scan rates) are rectangular in shape at low scan rates, but become paper-like with increasing scan rate. The decrease in specific capacitance at higher scanning rates is due to the incomplete reaction of the electrolyte and the rapid movement of ions.

Figure 5a shows the CV results of the supercapacitor cells fabricated using the pure alginate hydrogel electrolytes. All cells are observed to maintain their rectangular shape even at higher scanning rates. Among the cells, the pure alginate hydrogel has a rectangular shape at low scanning rates. The maximum specific capacitance of this cell is 3 mV/s, which decreases with increasing scan rates. Figure 5b shows that the maximum specific capacitance for A/P:P with 2.5 mL PEDOT:PSS decreases at a higher scan rate of 300 mV/s. In Figure 5c, supercapacitors made of alginate/PEDOT:PSS show a stable rectangular shape at higher scanning rates and a rate performance of 50% when the scan rate was increased to 300 mV s<sup>-1</sup>. The specific capacitance ( $C_s$ ) of the conductive A/P:P hydrogel can be calculated according to Equation (1) [46]:

$$C_s = \frac{I\Delta t}{\Delta V_m} \quad (1)$$

where  $I$  is the charge/discharge current,  $\Delta t$  is the discharge time,  $\Delta V$  is the electrochemical window, and  $m$  is the mass of the active material within the electrode [47].

The electrochemical behavior of the hydrogel treated with PEDOT:PSS (Figure 5c) shows slight differences in the shapes of the CV curves due to the high mobility of ions and electrons in A/P:P. In Figure 5b, a small change in the shape of the curve and a decrease in the capacitance of the electrolyte treated a ratio of 2.5 mL PEDOT:PSS indicates that the equivalent series resistance is low.

The results showed that the maximum specific capacitances of the alginate hydrogel with 2.5 and 5 mL PEDOT:PSS were 260 and 356 F/g at 100 mV/s, with energy density values of 36.15 and 40.08 W-h/kg at power densities of 100.05 and 400.35 W/kg, respectively. The observed specific capacitance for CV was superior to that reported for PEDOT:PSS-

based polymer electrolytes. These improvements are important for practical applications. In Table 1, a comparison of the reported work on hydrogels with the results in the present work is presented.

The performance of the hydrogels was tested using the GCD technique with a current density range of 30–200 mA g<sup>-1</sup>; the results are shown in Figure 6a,b. The figures show a discharge time that is equal to charge time. This is because of the presence of PEDOT:PSS, which facilitates the transport of charge carriers and increases the surface area. It can be inferred from the GCD curves that the electrode materials are reversed during the charging/discharging process, and the symmetrical curves indicate that the charging and discharging processes of the electrode materials are highly reversible.

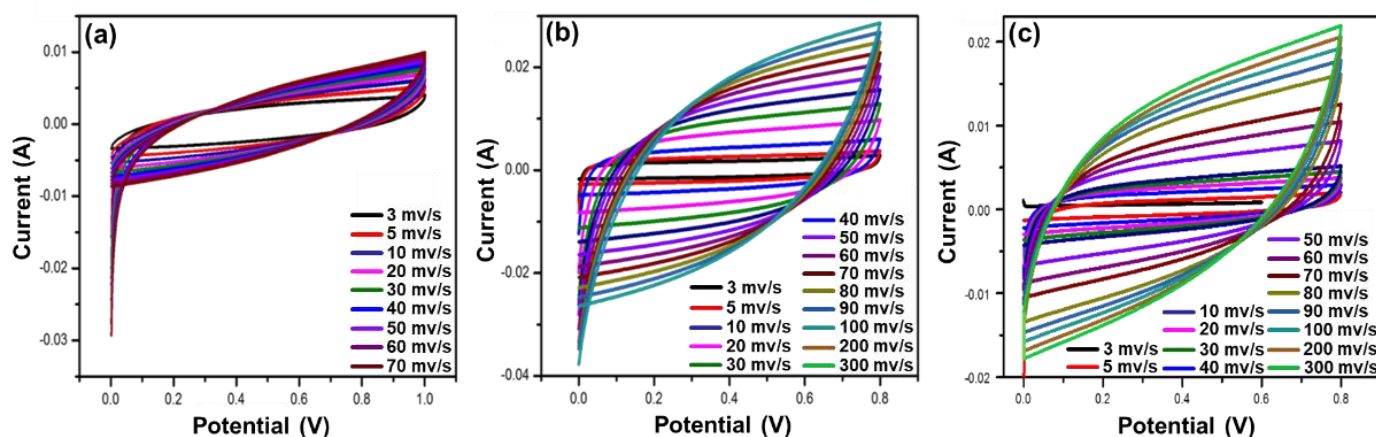


**Figure 5.** (a) CV curves of pure alginate hydrogel; (b) CV curves of pure alginate hydrogel with 2.5 mL PEDOT:PSS; and (c) CV curves of conductive alginate hydrogel with 5 mL PEDOT:PSS.

**Table 1.** Comparison of the electrochemical performance of the assembled supercapacitor with the previous work.

S. No	Materials	Applications	Capacity	Ref.
1.	Alginate/PEDOT:PSS	An energy storage device in portable and wearable electronic devices	Areal capacity 567.6 F.cm <sup>-3</sup> and 1002.4 mF.cm <sup>-2</sup> , large specific capacitance 246.4 mF.cm <sup>-2</sup> , high energy density of 21 μW.h.cm <sup>-2</sup>	[48]
2.	Soft alginic acid gel/PEDOT/PSS coated multi-walled carbon nanotubes (MWCNT)	Supercapacitors to modify the neural interface	Capacity of charge transfer observably increased from 0.5 mC/cm <sup>2</sup> to 1.2 mC/cm <sup>2</sup>	[49]
3.	PEDOT polymerized on N-doped carbon nanofibers (CNFs)	Supercapacitors	Exhibited a capacitance of 203 F g <sup>-1</sup> , nearly reaching its theoretical capacity of 210 F g <sup>-1</sup> , energy density of 97 μW-h cm <sup>-2</sup>	[50]
4.	PEDOT: PSS hydrogel film	Supercapacitors	158 F g <sup>-1</sup> at a scan rate of 50 mV s <sup>-1</sup> , cycling stability with 84.9% and capacitance retention after 2000 cycles.	[51]
5.	Alginic acid sodium salt/PEDOT:PSS	An aqueous supercapacitor	Exhibited high conductivity of 168.4 mS cm <sup>-1</sup>	[52]
6.	Alginate/PEDOT:PSS	A stable gel electrolyte membrane	356 F g <sup>-1</sup> at 100 mV/s g <sup>-1</sup> .	This work

To obtain further information about the capacity of the conductive alginate/PEDOT:PSS hydrogel in supercapacitors, EIS measurements were performed, as shown in Figure 7. The ionic conductivity of the conductive A/P:P hydrogel electrolyte was determined at 25 °C. Among all the synthesized hydrogel electrolytes, PEDOT:PSS made the hydrogels ionically conductive, as it enhanced the ionic conductivity owing to increased ionic diffusion across the hydrogel networks [53,54].

It can be seen in Figure 8a–c that the Nyquist plot confirms the capacitive behavior of A/P:P, with lower impedance at high frequencies and a gradient at low frequencies [55,56]. The room-temperature ionic conductivity of the as-prepared alginate hydrogel was found to be 10.5 × 10<sup>-3</sup> S cm<sup>-1</sup>. In Figure 8b,c, we note a high ionic conductivity, where conductive

A/P:P composite hydrogels with 2.5 and 5 mL of PEDOT:PSS achieved maximum ionic conductivities of  $11.2 \times 10^{-3}$ , and  $13.7 \times 10^{-3} \text{ S cm}^{-1}$ , respectively. This is because of the smooth transfer of charge carriers and electrolytic ions through water molecules around the charged groups [57], where the bulk resistance was calculated and the ionic conductivity was determined by means of the following equation:

$$\sigma = L/R_b A \tag{2}$$

where  $\sigma$  is the ionic conductivity ( $\text{S cm}^{-1}$ ), and L and A refer to the thickness (cm) and active area ( $\text{cm}^2$ ), respectively.

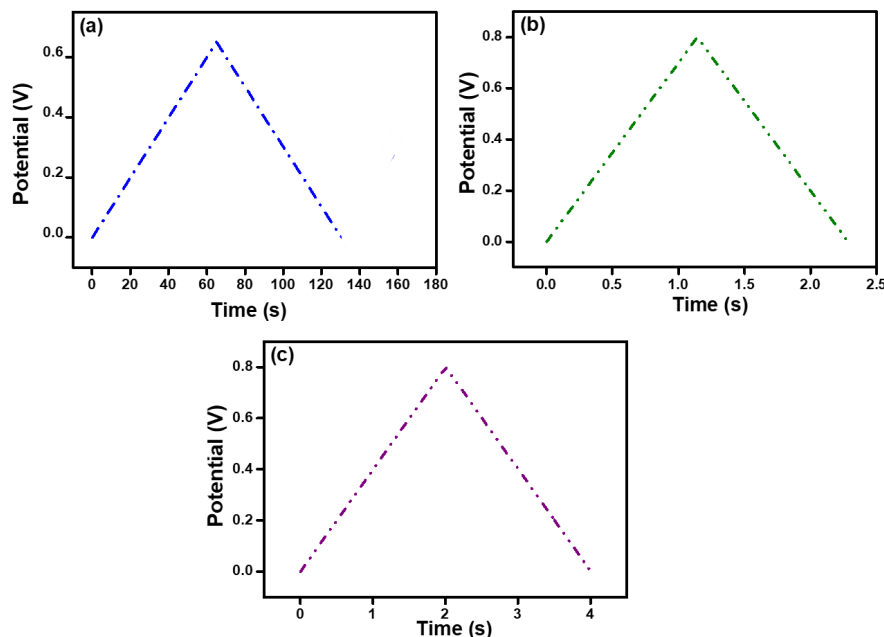


**Figure 6.** Galvanostatic charge–discharge (GCD) curves at 100 mA/g of (a) pure alginate hydrogel, (b) alginate hydrogel with 2.5 mL PEDOT:PSS, and (c) alginate hydrogel with 5 mL PEDOT:PSS.

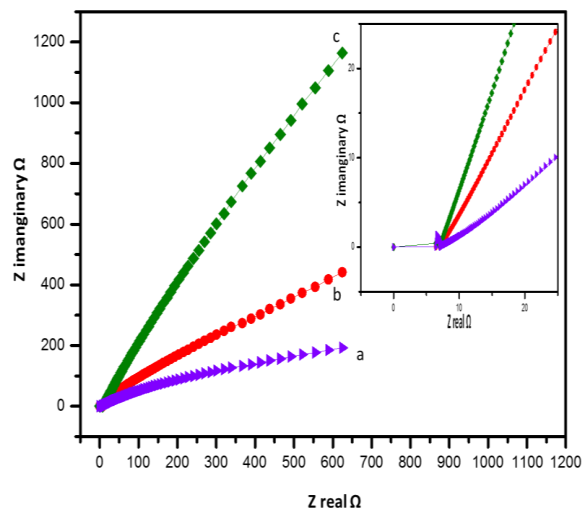


**Figure 7.** Nyquist plots of the (a) pure and (b,c) A/P:P composite hydrogel electrolytes.

### 2.7. Electrical Characterization Demonstrating the I-V

The hydrogel resistance (R) decreased with an increase in the PEDOT: PSS concentration. Increasing the ratio of PEDOT:PSS improves the electrical characteristics, as shown by the sharpest bend in Figure 9. This is most likely due to the electrophoretic method given by PEDOT-PSS to the pure non-conductive hydrogel [58]. This may be because the

higher electron diversity and electrical conductivity along the conductive hydrogel chains provided more efficient electron exchange. The 3D (A/P:P) compound treated with 5 mL PEDOT:PSS exhibited the lowest resistance [38].

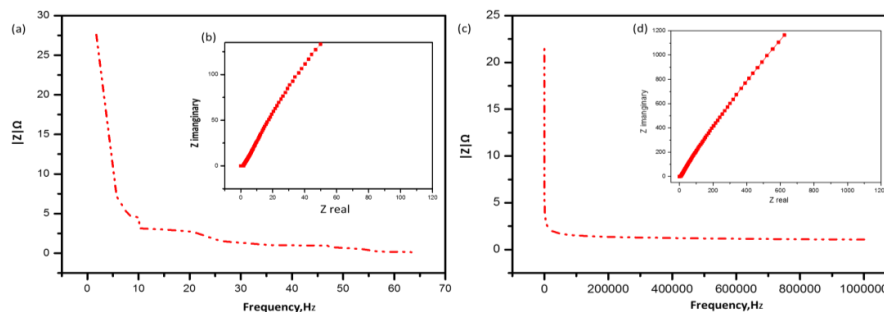


**Figure 8.** (a,c) Nyquist plots and (b,d) Bode plot of the conductive Alginate/PEDOT:PSS hydrogel electrolytes.

The sheet resistance of the conductive hydrogel (A/P:P) was determined, as shown in Table 2. All samples were cross-sectioned with an area of  $1 \times 1$  inches, and estimations were performed at room temperature using the four-line probe technique [59]. The imposed currents created a variable surface potential based on a four-line probe. This is a sufficiently robust and sensitive method for the determination of quartz. Hence, it was used to explore the spatial differences in the electronic conductivity and contact resistance of hydrogels (Figure 9b). Moreover, the four-line probe provides a larger contact area between the probe and A/P:P, while maintaining a small spacing between the lines that serve as the contacts. As shown in Figure 10, the current  $I$  and potential difference  $\Delta V$  are measured, and the apparent resistance  $R$  is calculated using Ohm's law  $R = \Delta V/I$  [60].

The linear relationship indicates the ideal conductivity in the case of high-concentration PEDOT:PSS, and we note the formation of a straight line passing through the origin. The A/P:P opposition was determined from the condition  $R_s = R(w/d)$ , where  $w$  is the width of the sample ( $w = 2.5$  cm) and ( $d = 0.35$  cm) is the line separation. As shown in Table 2, the conductive hydrogel exhibits a pattern similar to that of a stabilizing element. The inclusion of a small amount of PEDOT:PSS (2.5 mL) changes the pure hydrogel to a conductive state because of the arrangement of the associated PEDOT:PSS chains in the hydrogel mixture. The sheet resistance of the A/P:P samples diminishes from 3.5 to 0.9  $\Omega$ /square as the concentration of PEDOT:PSS increases from 2.5 to 5 mL of PEDOT:PSS [54].

The gel membrane formation process of organic PEDOT:PSS results in the formation of a 3D fibrous network, which plays a pivotal role in electrical conduction by providing efficient pathways for electrical conduction [55] treated with  $H_2SO_4$ . It can remove a part of the insulating PSS from the composite hydrogel A/P:P, which significantly improves the conductivity of the composite [61]. These changes in the estimations of sheet opposition can be attributed to the auxiliary dopant ( $H_2SO_4$ ), which causes morphological changes. These changes include expanding PEDOT-rich grains and producing a more slender PSS hindrance by specifically expelling PSS from the PEDOT:PSS film, prompting better charge transport pathways and associations between PEDOT-rich grains [38,58–62]. Moreover,  $H_2SO_4$  can also perform PEDOT:PSS installation on the hydrogel sample at room temperature to form a deeply regulated permeation conductive penetration by optimizing the bonds between the PEDOT:PSS chains and the hydrogel [63].

**Table 2.** Sheet resistance of (A/P:P) at different concentrations of PEDOT:PSS.

Rs ( $\Omega$ /Square)	Alginate Coating
3.5	2.5 mL PEDOT:PSS
0.9	5 mL PEDOT:PSS

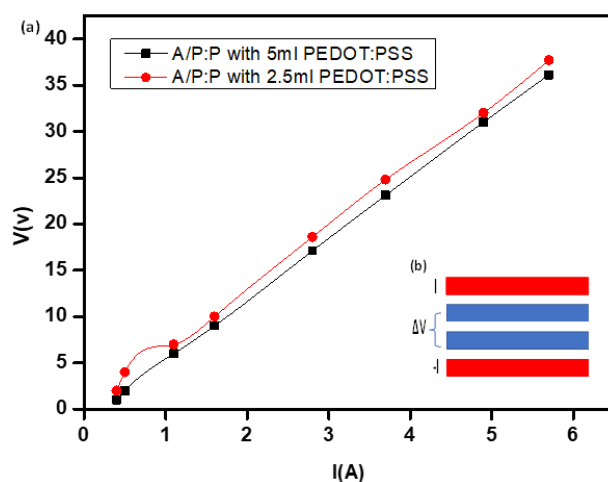


**Figure 9.** (a) I-V curve used for (A/P:P) at concentrations 2.5 and 5 mL of PEDOT:PSS. (b) Contact geometry for four-line probe where current  $I$  is injected and removed by the two outer contacts, and potential difference  $\Delta V$  is measured by the two inner contacts.

### 2.8. Self Healing and High Electrical Performance

Self healing is a desirable property that is evident in hydrogels possessing ionic bonds. These ionic bonds can be disturbed by stress, which can be reversed by electrostatic interactions between different charged components of ionic bonds, bridging the disruptions and leading to self-healing properties [38,53–62]. Herein, the self-healing properties of the as-prepared conductive A/P:P hydrogels were evaluated. The conductive A/P:P hydrogel possesses dynamic ionic interactions between the A/P:P carboxyl groups and hydrogen bonds, which are negatively charged gene chains formed by divalent ions [64]. In this study, a piece of conductive A/P:P hydrogel was used as a component of the circuit, and its functionality with respect to conductivity was tested. The results are shown in Figure 10a [65]. However, in step 2 (Figure 10b), realistic evidence of the self-healing ability of the hydrogel was demonstrated, wherein the hydrogel was cut in half with a scalpel. The separated pieces were then placed in contact to allow for independent self healing. It was observed that the pieces fused into one bulk piece again in less than 10 min [66]. Moreover, the ability of the self-healed hydrogel to illuminate the LED was demonstrated (Figure 10c), because the high ionic conductivity of the hydrogel was reinstated upon self healing, and was almost identical to  $\sigma = 13.7 \times 10^{-3} \text{ S cm}^{-1}$ . A comparison of the self-healing and high-electrification performances of supercapacitors with other devices described in the literature is shown in detail in Table 3.

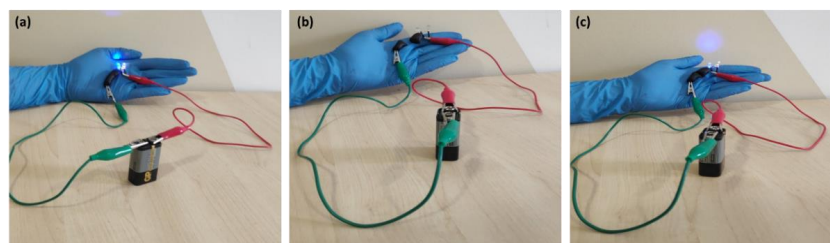


**Figure 10.** (a) LED is illuminated by a conductive hydrogel, (b) hydrogel being cut in half, and (c) hydrogel reinstated within 10 min of self healing.

Figure 11 shows the mechanical strength of the hydrogel before cutting by observing the self-healing efficiency when turning on the LED. When reconnecting the separate ends of a compound A/P:P with the ability to self heal, non-covalent interactions are formed again. LED illumination after the cut pieces were rejoined, providing strong evidence for the self-healing properties of the composite hydrogel. The electrochemical performance

was tested by CV before and after cutting the composite A/P:P hydrogel. Furthermore, the CV results demonstrated that the supercapacitor properties of the self-healing conductive A/P:P hydrogels were intact and reinstated once the healing process was completed.

The stress–strain response curves at 300 K along the armchair and zigzag thrusts are shown in Figure 12 relative to the precut specimen. The stress–strain behavior shows a linear correlation that approximately reaches the breaking strength point and terminates with decomposition, resulting in a brittle fracture of the sheet. However, for the sample after self healing, we notice a zigzag curve owing to the cut. Because of the elastic response of the bonds, the stress first shows a linear increasing trend with the stress, and then the bond angle and bond elongation change owing to the combined effect. The stress then exhibits nonlinear elasticity up to the critical value of stress. However, after self healing, we observe a phase shift that led to a simple non-uniform behavior–stress for oriented aliasing [67].

Hydrogel materials such as HPAAN/PDA have shown self healing times of 5 h and mechanical property recoveries of 67% in terms of tensile strain and 78% in terms of modulus [68–70].

**Table 3.** Comparing the self-healing and high-electrification performance of supercapacitors with other devices in the literature.

Fabrication	Method	Capacitance/Conductivity	Ref.
Poly(3,4-ethylenedioxythiophene) (PEDOT) and alginate	Making multifunctional conductive hydrogels using water-mediated self-assembly and polymerization techniques at room temperature for use as electrodes in supercapacitors. Because both polymers overlap, it is possible to combine the hydrogel's inherent biocompatibility and sustainability with its flexibility and self-healing abilities. The overlapping of both polymers allows flexibility and self-healing properties to be combined within the same hydrogel with the intrinsic biocompatibility and sustainability of these materials. The intercalation of both polymers allows the flexibility and self-healing properties to be combined within the same hydrogel with the intrinsic biocompatibility and sustainability of these materials. The electrochemical properties do not change significantly after several cut-off/self-healing cycles as observed by cyclic voltammetry. The electrochemical properties do not change significantly after a large number of cut-off/self-healing cycles, as observed by cyclic voltammetry.	Excellent capacitance values (35 mF cm <sup>-a</sup> )	[71]
Poly (N-acryloyl glycinamide-co-2-acrylamide-2-methylpropanesulfonic) (PNAGA-PAMPS) hydrogels with PEDOT/PSS	Simply through in situ doping, the specific conductivities of the hydrogels could be significantly enhanced by the doping of PEDOT/PSS. Due to the dynamic breakup and reconstruction of hydrogen bonds, cyclic heating and cooling may result in a reversible sol–gel transition and self-healing ability. The repaired hydrogels successfully regained conductivities as well as mechanical properties.	Conductivity values varies from 0.2 Sm <sup>-a</sup> to 2.2 Sm <sup>-1</sup>	[72]
Acrylamide (AAm), lauryl methacrylate (LMA), and 4-(6-(3-(6-(4-methyl-4-oxa-1,4-dihydropyrimidin-2-yl) ureido) hexylcarbamoyloxy) butyl acrylate (UPyHCBA)	A blade was used to cut the plate into two pieces, which were then joined together at 80 °C to study the self-healing capabilities of PU-PCL substrates. In order to perform the bending without fracturing the damaged area, the broken pieces of PU-PCL were reconnected. The tensile strength of a specimen after healing in comparison to its unhealed counterpart is a measure of healing effectiveness.	52.2 to 33.1 F g <sup>-2</sup>	[73]
CP's poly (3,4-ethylenedioxythiophene) (PEDOT)	Conducting polymeric hydrogels (CPHs) have successfully made a comeback as potential contenders for sensors, energy storage, bioelectronics, medical therapies, and treatments for environmental pollution. Due to their flexibility, CPHs offer a better framework for imagining cutting-edge technologies, including flexible electronic devices like supercapacitors. With a wider range of applications and the added benefit of a flexible synthetic process, PEDOT has emerged as a leading material in the field of bioelectronics.	Electrical conductivity (1–10 S cm <sup>-1</sup> )	[74]
PVA and PEDOT:PSS	A semi-interpenetrating polymer network (SIPN) strategy was used to create a set of flexible, stretchable, and conductive composite hydrogel composed of As. With increasing PEDOT:PSS content, the hydrogels' swelling ratio decreased. PVA networks with semi-interspersed PEDOT:PSS exhibited excellent tensile and compression properties as a result of the chemical crosslinking network and interactions between PVA and PEDOT:PSS. The hydrogels' electrical conductivity increased with increasing PEDOT:PSS content.	Conductive 4.5 × 10 <sup>-3</sup> S m <sup>-1</sup>	[75]

Table 3. Cont.

Fabrication	Method	Capacitance/Conductivity	Ref.
A sodium alginate/ $\text{Na}_2\text{SO}_4$	Combines sodium alginate (SA), borax, and hydrogen bonds between the amino acids in the gelatin chains and the SA to create a double-mesh conductive hydrogel. A phase change material (PCM), $\text{Na}_2\text{SO}_4 \cdot 10\text{H}_2\text{O}$ , was added to CH, which along with the borax's nucleation effect improved its ionic conductivity and temperature adaptability. CH exhibits an excellent elongation of 305.7% and a quick self-healing behavior in 60 s.	Capacitance of $185.3 \text{ F g}^{-1}$ ; resistance variation of $2.11 \Omega$	[76]
Polymer poly (3,4-ethylenedioxythiophene) polystyrenesulfonate (PEDOT: PSS) iota-carrageenan (CRG), polyvinyl alcohol (PVA)	Composition made of biopolymers through repeated freezing and thawing. The method, which is based on the creation of a polymer matrix after mixing CRG, PVA, and PEDOT: PSS, and the formation of a porous physical gel as a result of freezing and thawing cycles, is environmentally friendly. The resulting substance can swell in physiological solutions as well as distilled water and is stable in water.	Sheet conductivity was $0.01 \text{ [S cm}^{-1}\text{]}$ .	[43]

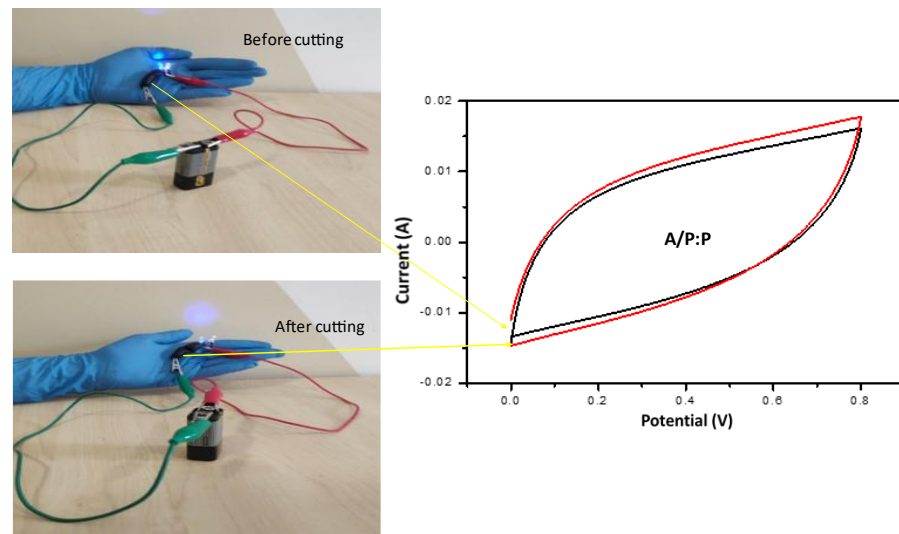


Figure 11. CV curves of self-healed conductive A/P:P hydrogel with high concentration of PEDOT:PSS, the black curve demonstrates the stress before cutting and the red one after cutting.

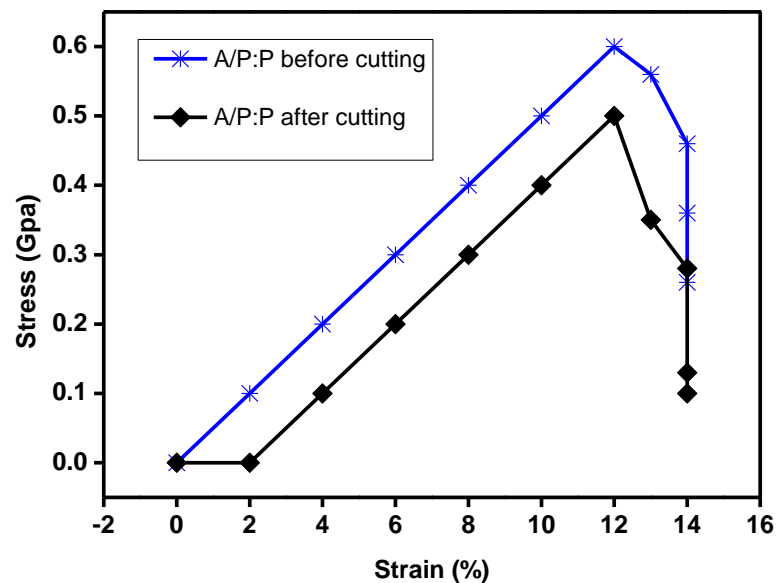


Figure 12. Tensile mechanical properties of hydrogel samples. Typical stress–strain curves for hydrogels and variation in elongation at fracture, hardness, and initial tensile modulus of A/P:P hydrogel with high concentration of PEDOT:PSS before cutting and after cutting, and the maximum stress with different values of  $x$ , respectively.

### 3. Experimental Section

#### 3.1. Materials

PEDOT:PSS (poly(3,4-ethylenedioxythiophene):poly(styrene sulfonate)) was bought from Osila, USA. Alginate powder ( $M_n = 357, 475$ ,  $M_n/M_w = 1.392$ ,  $M/G = 0.32$ ) was obtained from Sigma-Aldrich (St. Louis, MA, USA). Chemically pure sulfuric acid ( $H_2SO_4$ ) was purchased from Sigma-Aldrich (USA). A graphite conductive substrate was used as the electrode substrate, and it was coated with activated carbon (surface area: 1800–2000  $m^2/g$ , particle size: 5–20  $\mu m$ ) from Sigma Aldrich. Deionized (DI) water was used as the solvent.

#### 3.2. Preparation of Self-Healing Alginate/PEDOT:PSS(A/P:P) Hydrogel Electrolyte

Initially, pure alginate hydrogel was prepared by the following process: 1 g of alginate was dissolved in 50 mL of water, stirred at 60 °C for 1 h using a magnetic stirrer to form a transparent solution. A  $H_2SO_4$  solution (2.0 mol/L) was added to start the polymerization reaction. The reaction was carried out for 1 h at 60 °C, as shown in Figure 13A. The self-healable alginate/PEDOT:PSS hydrogel electrolyte was prepared as follows: To begin with, 1 g of alginate was dissolved in 50 mL water, while stirring at 60 °C for 1 h to form a transparent solution. Then, aqueous PEDOT:PSS (2.5 mL) was added to the above solution with vigorous stirring until a bluish-black homogeneous mixture was obtained. The solutions were then added to glass tubes, to which  $H_2SO_4$  solution (2.0 mol/L) was added to initiate the polymerization reaction. The reaction was carried out for 1 h at 60 °C, and a hydrogel was obtained (Figure 13B). In Figure 13C, we repeat the same steps as in B, but increasing the PEDOT:PSS ratio to 5 mL. By controlling the appropriate amount of PEDOT:PSS, the order, shape, and coherence of the sample can be maintained. Moreover, the strong bonding between the conductive domains rich in PEDOT:PSS and alginate provides excellent electrical conductivity and aqueous stability. Table 4 lists the detailed compositions of the prepared samples.

PEDOT polymerizes in the presence of alginate to produce porous alginate conductive PEDOT scaffolds, resulting in the synthesis of electrically conductive alginate/PEDOT:PSS within a block matrix using  $H_2SO_4$ .  $H_2SO_4$  causes chemical crosslinking of PEDOT:PSS with alginate. These compounds demonstrate great potential in the fields of tissue engineering and elastomeric reversible materials. This potential arises from their adequate cellular compatibility and simplicity of manipulation through the chemical crosslinking of PEDOT:PSS with alginate as a result of  $H_2SO_4$  usage. An alginate/PEDOT:PSS hydrogel was formed when the hydrogel electrolyte was treated with  $H_2SO_4$  acid to create 3D hydrogels. This process is called “crystallization”, because it causes the material to acquire a stacked, interlocking nanostructure. In contrast, PEDOT:PSS with sulfuric acid dissolves PSS and produces nanofibers of PEDOT through a structural transition mechanism that resembles grains. The conductivity of the crosslinked alginate/PEDOT:PSS hydrogel can be improved by  $H_2SO_4$  crystallization while maintaining its stability and cytocompatibility. PEDOT:PSS is perfect for the crosslinking solidification process, which allows for the control of pore size, quantity, and orientation because it is water-dispersible. Additionally, the hydrogel exhibited significantly improved flexibility and conductivity, while maintaining biocompatibility. By extending the binary system, PEDOT:PSS-based ternary composite films can become high-performance materials with several benefits. When the nanoparticles were dispersed in PEDOT:PSS solutions, they formed dense interlocking channels that decreased the interchain distance and consequently increased the conductivity of the resulting film. PEDOT:PSS primarily serves as a binder to encapsulate binary hybrids. High-strength supramolecular polymer conductive hydrogels were created that were crosslinked by a single amide hydrogen bond and strengthened [6,77,78].

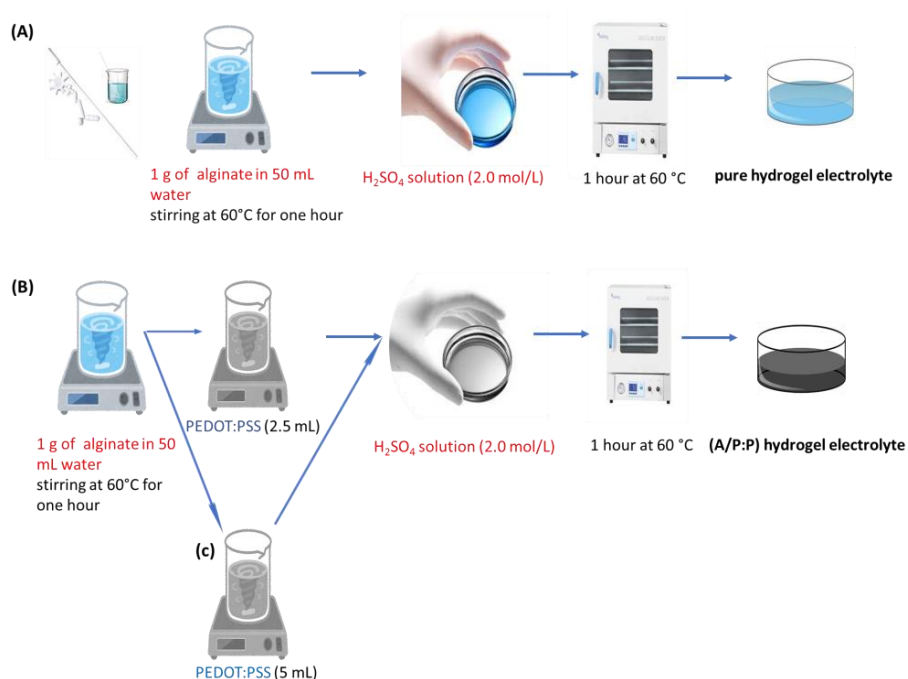


**Figure 13.** Preparation of (A) pure alginate and (B,C) alginate/PEDOT:PSS (A/P:P) hydrogel electrolytes.

**Table 4.** Details of the A/P:P with respect to the PEDOT:PSS ratio.

System	Details
A-Pure alginate hydrogel	(1 g alginate + 50 mL of water) + 2.0 mol/L H <sub>2</sub> SO <sub>4</sub>
B-A/P:P	2.5 mL PEDOT:PSS + pure alginate hydrogel solution+2.0 mol/L H <sub>2</sub> SO <sub>4</sub> .
C-A/P:P	5ml PEDOT:PSS + pure alginate hydrogel solution+2.0 mol/L H <sub>2</sub> SO <sub>4</sub> .

### 3.3. Fabrication of Electrode

Carbon slurry was used to construct the working electrode. This slurry was prepared by adding 80:10:10 mass percentages of activated carbon, carbon black, and poly (vinylidene fluoride) binder, respectively, to N-methyl-2-pyrrolidone solvent. To ensure homogeneity, the mixture was stirred continuously for a few hours at RT. The slurry was then applied to the activated carbon and left to dry for 1 h at 100 °C.

### 3.4. Fabrication of Smart Flexible Electrochemical Supercapacitor

The working electrode substrate was prepared as follows:

A conductive graphite substrate was coated with activated carbon black by dispersing an appropriate amount of graphite sheets. The electrode substrate was obtained by drying for 1 h at a temperature of 100 °C. For the assembly of the bipolar supercapacitor device, the hydrogel was first squarely cut to a size of 2 cm × 2 cm and used simultaneously as an electrolyte and separator. Subsequently, a smart flexible supercapacitor was assembled by sandwiching the hydrogel electrolyte between the prepared electrodes (electrode/hydrogel electrolyte/electrode).

### 3.5. Characterization

#### 3.5.1. Structural and Morphological Analyses

The surface morphology was studied using field-emission scanning electron microscopy (SEM (JEOL, JSM-6380LA)) with an accelerating voltage of 5 kV. The samples

were coated with gold before conducting SEM analysis. The structural characterization of the pure and synthesized hydrogels was performed using Fourier-transform infrared spectroscopy (FTIR). A Nicolet iS50 FTIR spectrometer (Thermo Fisher Scientific Co. (Waltham, MA, USA)) was used to record the FTIR spectra of the pure and synthesized alginate hydrogels. The spectral range and resolution factor of the FTIR spectrometer ranged from 500 to 4000  $\text{cm}^{-1}$ . The X-ray diffraction (XRD) patterns of the porous alginate hydrogels and A/P:P were obtained using Cu-K $\alpha$  radiation (1.5406 Å) at a current of 30 mA, voltage of 40 kV, and scanning angle  $2\theta$  over a step size of 0.02/s.

### 3.5.2. Electrochemical Studies of Electrolyte and Supercapacitor

The ionic conductivity ( $\sigma$ ) of the alginate/PEDOT:PSS hydrogel electrolyte was estimated using an impedance spectroscopic instrument Hioki 3532-50 LCR HiTESTER over a frequency range of 50 Hz to 5 MHz. Electrochemical studies were performed for electrochemical cells, which were prepared by sandwiching the as-prepared polymer hydrogel (alginate/PEDOT:PSS) electrolyte between activated carbon materials coated with graphite electrodes. CV, galvanostatic charge–discharge (GCD), and electrochemical impedance spectroscopy (EIS) on alginate/PEDOT:PSS hydrogel electrolytes were performed using a Gamry Interface 1000. To investigate the electrical properties of the conductive hydrogels, a four-line probe method was used. The electrical resistance of the hydrogel synthesized from I-V bends was determined at a temperature of 25 °C. The electrical resistance (R) of each gel was measured during drying using a four-line probe method. The resistance of the plate was determined using the following equation [42]:

$$R_s = R\left(\frac{w}{d}\right) \quad (3)$$

where  $w$  is the width of the sample (2.5 cm) and  $d$  is the spacer between the leads (0.35 cm).

### 3.5.3. Tensile Test

Tensile testing was performed using an Instron 3360 electronic universal testing device (Instron Corporation, Norfolk County, MA, USA). The prepared specimens were cut into rectangular shapes according to the JISK6251-7 standard size (length 2 cm, width 0.5 cm, gauge length 0.5 mm).

## 4. Conclusions

In summary, the present study aimed to analyze the self-healing properties of semi-IPN hydrogels based on PEDOT:PSS with the additive  $\text{H}_2\text{SOH}_3\text{SO}_2$ . We developed a facile and scalable protocol for the preparation of conductive flexible alginate/PEDOT:PSS hydrogels with tunable 3D microstructures as electrically active materials for high-performance flexible solid-state supercapacitors. A/P:P hydrogel capacitors were successfully synthesized by employing  $\text{H}_2\text{SO}_4$  as an initiator to yield a polymeric alginate hydrogel with PEDOT:PSS encapsulated within the matrices, which was employed as an electrolyte for the supercapacitor. Analysis of the structure and surface morphology of the pure and synthesized hydrogels were performed using Fourier-transform infrared (FTIR) spectroscopy and scanning electron microscopy (SEM), respectively. The symmetric alginate with 5 mL of the PEDOT:PSS-based flexible supercapacitor achieved a specific capacitance of 356 F/g at 100 mV/s (energy density of 40.08 Wh/kg at a power density of 400.35 W/kg) at 100 mV/s  $\text{g}^{-1}$  and sheet resistance of 0.9  $\Omega$ /square. The ionic conductivity was measured at 25 °C and was found to be high, i.e.,  $13.7 \times 10^{-3} \text{ S cm}^{-1}$ . The as-prepared alginate/PEDOT:PSS hydrogel displayed conductive properties, and had the potential to achieve rapid self healing.

**Author Contributions:** Conceptualization, N.M.B., K.R. and S.F.A.; methodology, N.M.B., K.R., M.R.S. and S.F.A.; validation, M.B., S.R. and M.R.S.; formal analysis, M.B., M.K. (Mufsir Kuniyil) and B.S.; investigation, M.B., S.R., M.R.S. and M.K. (Mujeeb Khan); data curation, M.R.S. and M.K. (Mujeeb Khan); writing—original draft preparation, N.M.B., K.R. and S.F.A.; writing—review and

editing, N.M.B., K.R., M.K. (Mufsir Kuniyil) and S.F.A.; supervision, S.F.A.; funding acquisition, M.R.S. All authors have read and agreed to the published version of the manuscript.

**Funding:** Researchers Supporting Project number (RSPD2023R665), King Saud University, Riyadh, Saudi Arabia.

**Institutional Review Board Statement:** Not applicable.

**Data Availability Statement:** Data is contained within the article.

**Acknowledgments:** The authors acknowledge the funding from Researchers Supporting Project number (RSPD2023R665), King Saud University, Riyadh, Saudi Arabia.

**Conflicts of Interest:** The authors declare no conflict of interest.

## References

- Spanneberg, R.; Osswald, F.; Kolesov, I.; Anton, W.; Radusch, H.-J.; Glomb, M.A. Model Studies on Chemical and Textural Modifications in Gelatin Films by Reaction with Glyoxal and Glycolaldehyde. *J. Agric. Food Chem.* **2010**, *58*, 3580–3585. [[CrossRef](#)] [[PubMed](#)]
- Wang, B.; Wu, X.; Li, J.; Hao, X.; Lin, J.; Cheng, D.; Lu, Y. Thermosensitive Behavior and Antibacterial Activity of Cotton Fabric Modified with a Chitosan-poly(N-isopropylacrylamide) Interpenetrating Polymer Network Hydrogel. *Polymers* **2016**, *8*, 110. [[CrossRef](#)] [[PubMed](#)]
- Liu, Y.; Jiang, S.P.; Shao, Z. Intercalation pseudocapacitance in electrochemical energy storage: Recent advances in fundamental understanding and materials development. *Mater. Today Adv.* **2020**, *7*, 100072. [[CrossRef](#)]
- Yu, X.; Lu, B.; Xu, Z. Super Long-Life Supercapacitors Based on the Construction of Nanohoneycomb-Like Strongly Coupled CoMoO<sub>4</sub>-3D Graphene Hybrid Electrodes. *Adv. Mater.* **2014**, *26*, 1044–1051. [[CrossRef](#)]
- Bashir, S.; Hina, M.; Iqbal, J.; Rajpar, A.H.; Mujtaba, M.A.; Alghamdi, N.A.; Wageh, S.; Ramesh, K.; Ramesh, S. Fundamental Concepts of Hydrogels: Synthesis, Properties, and Their Applications. *Polymers* **2020**, *12*, 2702. [[CrossRef](#)] [[PubMed](#)]
- Kim, K.; Park, J.; Lee, J.; Suh, S.; Kim, W. Ultrafast PEDOT:PSS/H<sub>2</sub>SO<sub>4</sub> Electrical Double Layer Capacitors: Comparison with PANI Pseudocapacitors. *ChemSusChem* **2022**. [[CrossRef](#)]
- Chen, C.-R.; Qin, H.; Cong, H.-P.; Yu, S.-H. A Highly Stretchable and Real-Time Healable Supercapacitor. *Adv. Mater.* **2019**, *31*, 1900573. [[CrossRef](#)]
- Yoo, H.D.; Markevich, E.; Salitra, G.; Sharon, D.; Aurbach, D. On the challenge of developing advanced technologies for electrochemical energy storage and conversion. *Mater. Today* **2014**, *17*, 110–121. [[CrossRef](#)]
- Salanne, M.; Rotenberg, B.; Naoi, K.; Kaneko, K.; Taberna, P.L.; Grey, C.P.; Dunn, B.; Simon, P. Efficient storage mechanisms for building better supercapacitors. *Nat. Energy* **2016**, *1*, 16070. [[CrossRef](#)]
- Irzhak, V.I.; Uflyand, I.E.; Dzhardimalieva, G.I. Self-Healing of Polymers and Polymer Composites. *Polymers* **2022**, *14*, 5404. [[CrossRef](#)]
- Foteinidis, G.; Kosarli, M.; Nikiphorides, P.; Tzirka, K.; Paipetis, A.S. Capsule-Based Self-Healing and Self-Sensing Composites with Enhanced Mechanical and Electrical Restoration. *Polymers* **2022**, *14*, 5264. [[CrossRef](#)]
- Cheong, M.; Zhitomirsky, I. Electrodeposition of alginic acid and composite films. *Colloids Surf. A* **2008**, *328*, 73–78. [[CrossRef](#)]
- Platonova, E.; Ponomareva, P.; Lokiaeava, Z.; Pavlov, A.; Nelyub, V.; Polezhaev, A. New Building Blocks for Self-Healing Polymers. *Polymers* **2022**, *14*, 5394. [[CrossRef](#)]
- Rumon, M.M.H.; Akib, A.A.; Sultana, F.; Moniruzzaman, M.; Niloy, M.S.; Shakil, M.S.; Roy, C.K. Self-Healing Hydrogels: Development, Biomedical Applications, and Challenges. *Polymers* **2022**, *14*, 4539. [[CrossRef](#)]
- Huang, Y.; Zhong, M.; Huang, Y.; Zhu, M.; Pei, Z.; Wang, Z.; Xue, Q.; Xie, X.; Zhi, C. A self-healable and highly stretchable supercapacitor based on a dual crosslinked polyelectrolyte. *Nat. Commun.* **2015**, *6*, 10310. [[CrossRef](#)]
- Saxena, A.; Sharda, S.; Kumar, S.; Kumar, B.; Shirodkar, S.; Dahiya, P.; Sahney, R. Synthesis of Alginate Nanogels with Polyvalent 3D Transition Metal Cations: Applications in Urease Immobilization. *Polymers* **2022**, *14*, 1277. [[CrossRef](#)] [[PubMed](#)]
- Elbayomi, S.M.; Wang, H.; Tamer, T.M.; You, Y. Enhancement of Antioxidant and Hydrophobic Properties of Alginate via Aromatic Derivatization: Preparation, Characterization, and Evaluation. *Polymers* **2021**, *13*, 2575. [[CrossRef](#)] [[PubMed](#)]
- Jin, X.; Sun, G.; Zhang, G.; Yang, H.; Xiao, Y.; Gao, J.; Zhang, Z.; Qu, L. A cross-linked polyacrylamide electrolyte with high ionic conductivity for compressible supercapacitors with wide temperature tolerance. *Nano Res.* **2019**, *12*, 1199–1206. [[CrossRef](#)]
- Matricardi, P.; Di Meo, C.; Coviello, T.; Hennink, W.E.; Alhaique, F. Interpenetrating Polymer Networks polysaccharide hydrogels for drug delivery and tissue engineering. *Adv. Drug Deliv. Rev.* **2013**, *65*, 1172–1187. [[CrossRef](#)]
- Yang, Z.; Deng, J.; Chen, X.; Ren, J.; Peng, H. A Highly Stretchable, Fiber-Shaped Supercapacitor. *Angew. Chem. Int. Ed.* **2013**, *52*, 13453–13457. [[CrossRef](#)]
- Wang, Q.-Q.; Liu, Y.; Zhang, C.-J.; Zhang, C.; Zhu, P. Alginate/gelatin blended hydrogel fibers cross-linked by Ca<sup>2+</sup> and oxidized starch: Preparation and properties. *Mater. Sci. Eng. C* **2019**, *99*, 1469–1476. [[CrossRef](#)]
- Ikura, R.; Park, J.; Osaki, M.; Yamaguchi, H.; Harada, A.; Takashima, Y. Design of self-healing and self-restoring materials utilizing reversible and movable crosslinks. *NPG Asia Mater.* **2022**, *14*, 10. [[CrossRef](#)]

23. Meen, T.-H.; Chen, K.-L.; Chen, Y.-H.; Chen, W.-R.; Chou, D.-W.; Lan, W.-H.; Huang, C.-J. The Effects of Dilute Sulfuric Acid on Sheet Resistance and Transmittance in Poly(3,4-thylenedioxythiophene): Poly(styrenesulfonate) Films. *Int. J. Photoenergy* **2013**, *2013*, 843410. [[CrossRef](#)]
24. Gao, N.; Yu, J.; Tian, Q.; Shi, J.; Zhang, M.; Chen, S.; Zang, L. Application of PEDOT:PSS and Its Composites in Electrochemical and Electronic Chemosensors. *Chemosensors* **2021**, *9*, 79. [[CrossRef](#)]
25. Shen, Z.; Zhang, Z.; Zhang, N.; Li, J.; Zhou, P.; Hu, F.; Rong, Y.; Lu, B.; Gu, G. High-Stretchability, Ultralow-Hysteresis Conducting Polymer Hydrogel Strain Sensors for Soft Machines. *Adv. Mater.* **2022**, *34*, 2203650. [[CrossRef](#)]
26. Zhang, C.; Wang, M.; Jiang, C.; Zhu, P.; Sun, B.; Gao, Q.; Gao, C.; Liu, R. Highly adhesive and self-healing  $\gamma$ -PGA/PEDOT:PSS conductive hydrogels enabled by multiple hydrogen bonding for wearable electronics. *Nano Energy* **2022**, *95*, 106991. [[CrossRef](#)]
27. Hu, F.; Xue, Y.; Xu, J.; Lu, B. PEDOT-Based Conducting Polymer Actuators. *Front. Robot. AI* **2019**, *6*. [[CrossRef](#)]
28. Zhang, M.; Zhou, Q.; Chen, J.; Yu, X.; Huang, L.; Li, Y.; Li, C.; Shi, G. An ultrahigh-rate electrochemical capacitor based on solution-processed highly conductive PEDOT:PSS films for AC line-filtering. *Energy Environ. Sci.* **2016**, *9*, 2005–2010. [[CrossRef](#)]
29. Kuang, X.; Arıcan, M.O.; Zhou, T.; Zhao, X.; Zhang, Y.S. Functional Tough Hydrogels: Design, Processing, and Biomedical Applications. *Acc. Mater. Res.* **2022**. [[CrossRef](#)]
30. Song, J.; Ma, G.; Qin, F.; Hu, L.; Luo, B.; Liu, T.; Yin, X.; Su, Z.; Zeng, Z.; Jiang, Y.; et al. High-Conductivity, Flexible and Transparent PEDOT:PSS Electrodes for High Performance Semi-Transparent Supercapacitors. *Polymers* **2020**, *12*, 450. [[CrossRef](#)]
31. Hina, M.; Bashir, S.; Kamran, K.; Iqbal, J.; Ramesh, S.; Ramesh, K. Fabrication of aqueous solid-state symmetric supercapacitors based on self-healable poly (acrylamide)/PEDOT:PSS composite hydrogel electrolytes. *Mater. Chem. Phys.* **2021**, *273*, 125125. [[CrossRef](#)]
32. Lin, J.; Zheng, S.Y.; Xiao, R.; Yin, J.; Wu, Z.L.; Zheng, Q.; Qian, J. Constitutive behaviors of tough physical hydrogels with dynamic metal-coordinated bonds. *J. Mech. Phys. Solids* **2020**, *139*, 103935. [[CrossRef](#)]
33. Łabowska, M.B.; Cierluk, K.; Jankowska, A.M.; Kulbacka, J.; Detyna, J.; Michalak, I. A Review on the Adaption of Alginate-Gelatin Hydrogels for 3D Cultures and Bioprinting. *Materials* **2021**, *14*, 858. [[CrossRef](#)] [[PubMed](#)]
34. Zhang, S.; Chen, Y.; Liu, H.; Wang, Z.; Ling, H.; Wang, C.; Ni, J.; Çelebi-Saltik, B.; Wang, X.; Meng, X.; et al. Room-Temperature-Formed PEDOT:PSS Hydrogels Enable Injectable, Soft, and Healable Organic Bioelectronics. *Adv. Mater.* **2020**, *32*, 1904752. [[CrossRef](#)]
35. Bode, F.; da Silva, M.A.; Drake, A.F.; Ross-Murphy, S.B.; Dreiss, C.A. Enzymatically Cross-Linked Tilapia Gelatin Hydrogels: Physical, Chemical, and Hybrid Networks. *Biomacromolecules* **2011**, *12*, 3741–3752. [[CrossRef](#)]
36. Ouyang, J. Recent advances of intrinsically conductive polymers. *Acta Phys. Chim. Sin.* **2018**, *34*, 1211–1220. [[CrossRef](#)]
37. Sakai, S.; Yamaguchi, S.; Takei, T.; Kawakami, K. Oxidized Alginate-Cross-Linked Alginate/Gelatin Hydrogel Fibers for Fabricating Tubular Constructs with Layered Smooth Muscle Cells and Endothelial Cells in Collagen Gels. *Biomacromolecules* **2008**, *9*, 2036–2041. [[CrossRef](#)]
38. Maeda, R.; Shinohara, Y.; Kawakami, H.; Isoda, Y.; Kanazawa, I.; Mitsuishi, M. The conducting fibrillar networks of a PEDOT:PSS hydrogel and an organogel prepared by the gel-film formation process. *Nanotechnology* **2021**, *32*, 135403. [[CrossRef](#)]
39. Guo, X.; Huang, Y.; Wu, C.; Mao, L.; Wang, Y.; Xie, Z.; Liu, C.; Zhang, Y. Flexible and reversibly deformable radio-frequency antenna based on stretchable SWCNTs/PANI/Lycra conductive fabric. *Smart Mater. Struct.* **2017**, *26*, 105036. [[CrossRef](#)]
40. Yang, Z.; Pang, Y.; Han, X.-l.; Yang, Y.; Ling, J.; Jian, M.; Zhang, Y.; Yang, Y.; Ren, T.-L. Graphene Textile Strain Sensor with Negative Resistance Variation for Human Motion Detection. *ACS Nano* **2018**, *12*, 9134–9141. [[CrossRef](#)]
41. Hu, L.; Pasta, M.; La Mantia, F.; Cui, L.; Jeong, S.; Deshazer, H.D.; Choi, J.W.; Han, S.M.; Cui, Y. Stretchable, Porous, and Conductive Energy Textiles. *Nano Lett.* **2010**, *10*, 708–714. [[CrossRef](#)]
42. Flygare, J.D.; Riet, A.A.; Mazzeo, B.A.; Wheeler, D.R. Mathematical Model of Four-Line Probe to Determine Conductive Properties of Thin-Film Battery Electrodes. *J. Electrochem. Soc.* **2015**, *162*, A2136. [[CrossRef](#)]
43. Gotovtsev, P.M.; Badranova, G.U.; Zubavichus, Y.V.; Chumakov, N.K.; Antipova, C.G.; Kamyshinsky, R.A.; Presniakov, M.Y.; Tokaev, K.V.; Grigoriev, T.E. Electroconductive PEDOT:PSS-based hydrogel prepared by freezing-thawing method. *Heliyon* **2019**, *5*, e02498. [[CrossRef](#)]
44. Peng, J.; Wang, X.; Lou, T. Preparation of chitosan/gelatin composite foam with ternary solvents of dioxane/acetic acid/water and its water absorption capacity. *Polym. Bull.* **2020**, *77*, 5227–5244. [[CrossRef](#)]
45. Teo, M.Y.; RaviChandran, N.; Kim, N.; Kee, S.; Stuart, L.; Aw, K.C.; Stringer, J. Direct Patterning of Highly Conductive PEDOT:PSS/Ionic Liquid Hydrogel via Microreactive Inkjet Printing. *ACS Appl. Mater. Interfaces* **2019**, *11*, 37069–37076. [[CrossRef](#)]
46. Chen, X.; Fang, S.; Hou, Z. Preparation and research progress of polymer-based flexible conductive composites. *J. Polym. Sci. Eng.* **2018**, *1*, 243. [[CrossRef](#)]
47. Dalton, A.B.; Collins, S.; Razal, J.; Munoz, E.; Ebron, V.H.; Kim, B.G.; Coleman, J.N.; Ferraris, J.P.; Baughman, R.H. Continuous carbon nanotube composite fibers: Properties, potential applications, and problems. *J. Mater. Chem.* **2004**, *14*, 1–3. [[CrossRef](#)]
48. Wang, P.; Du, X.; Wang, X.; Zhang, K.; Sun, J.; Chen, Z.; Xia, Y. Integrated fiber electrodes based on marine polysaccharide for ultrahigh-energy-density flexible supercapacitors. *J. Power Sources* **2021**, *506*, 230130. [[CrossRef](#)]
49. Wang, K.; Tian, L.; Wang, T.; Zhang, Z.; Gao, X.; Wu, L.; Fu, B.; Liu, X. Electrodeposition of alginate with PEDOT/PSS coated MWCNTs to make an interpenetrating conducting hydrogel for neural interface. *Compos. Interfaces* **2019**, *26*, 27–40. [[CrossRef](#)]

50. Zhu, X.; Han, X.; Guo, R.; Yuan, P.; Dang, L.; Liu, Z.; Lei, Z. Vapor-phase polymerization of fibrous PEDOT on carbon fibers film for fast pseudocapacitive energy storage. *Appl. Surf. Sci.* **2022**, *597*, 153684. [[CrossRef](#)]
51. Xu, D.; Feng, X.; Niu, D.; Zhu, X.; Song, Y. PEDOT: PSS hydrogel film for supercapacitors via  $AlCl_3$ -induced cross-linking and subsequent organic solvent treatments. *Mater. Today Commun.* **2020**, *24*, 101090. [[CrossRef](#)]
52. Ji, D.; Park, J.M.; Oh, M.S.; Nguyen, T.L.; Shin, H.; Kim, J.S.; Kim, D.; Park, H.S.; Kim, J. Superstrong, superstiff, and conductive alginate hydrogels. *Nat. Commun.* **2022**, *13*, 3019. [[CrossRef](#)] [[PubMed](#)]
53. Huang, Y.; Wang, Y.; Gao, L.; He, X.; Liu, P.; Liu, C. Characterization of stretchable SWCNTs/Lycra fabric electrode with dyeing process. *J. Mater. Sci.-Mater. Electron.* **2017**, *28*, 4279–4287. [[CrossRef](#)]
54. Lu, Y.; Li, Y.; Pan, J.; Wei, P.; Liu, N.; Wu, B.; Cheng, J.; Lu, C.; Wang, L. Poly(3,4-ethylenedioxythiophene)/poly(styrenesulfonate)-poly(vinyl alcohol)/poly(acrylic acid) interpenetrating polymer networks for improving optrode-neural tissue interface in optogenetics. *Biomaterials* **2012**, *33*, 378–394. [[CrossRef](#)]
55. Guo, X.; Li, J.; Wang, F.; Zhang, J.-H.; Zhang, J.; Shi, Y.; Pan, L. Application of conductive polymer hydrogels in flexible electronics. *J. Polym. Sci.* **2022**, *60*, 2635–2662. [[CrossRef](#)]
56. Mir, A.; Kumar, A.; Riaz, U. A short review on the synthesis and advance applications of polyaniline hydrogels. *RSC Adv.* **2022**, *12*, 19122–19132. [[CrossRef](#)]
57. Qian, X.; Gu, N.; Cheng, Z.; Yang, X.; Wang, E.; Dong, S. Methods to study the ionic conductivity of polymeric electrolytes using a.c. impedance spectroscopy. *J. Solid State Electrochem.* **2001**, *6*, 8–15. [[CrossRef](#)]
58. Abidian, M.R.; Corey, J.M.; Kipke, D.R.; Martin, D.C. Conducting-Polymer Nanotubes Improve Electrical Properties, Mechanical Adhesion, Neural Attachment, and Neurite Outgrowth of Neural Electrodes. *Small* **2010**, *6*, 421–429. [[CrossRef](#)]
59. Weinbach, Q.; Thakkar, S.V.; Carvalho, A.; Chaplais, G.; Combet, J.; Constantin, D.; Stein, N.; Collin, D.; Biniek, L. Efficient Control of a Mesoporous Fibrillar PEDOT:PSS Aerogel Structure for Promising Thermoelectric Applications. *Front. Electron. Mater.* **2022**, *2*, 875856. [[CrossRef](#)]
60. Lanterman, B.J.; Riet, A.A.; Gates, N.S.; Flygare, J.D.; Cutler, A.D.; Vogel, J.E.; Wheeler, D.R.; Mazzeo, B.A. Micro-Four-Line Probe to Measure Electronic Conductivity and Contact Resistance of Thin-Film Battery Electrodes. *J. Electrochem. Soc.* **2015**, *162*, A2145. [[CrossRef](#)]
61. Li, L.; Zhang, N.; Zhang, M.; Zhang, X.; Zhang, Z. Flexible  $Ti_3C_2T_x$ /PEDOT:PSS films with outstanding volumetric capacitance for asymmetric supercapacitors. *Dalton Trans.* **2019**, *48*, 1747–1756. [[CrossRef](#)]
62. Cai, Z.; Martin, C.R. Electronically conductive polymer fibers with mesoscopic diameters show enhanced electronic conductivities. *J. Am. Chem. Soc.* **1989**, *111*, 4138–4139. [[CrossRef](#)]
63. Shi, Y.; Wang, M.; Ma, C.; Wang, Y.; Li, X.; Yu, G. A Conductive Self-Healing Hybrid Gel Enabled by Metal–Ligand Supramolecule and Nanostructured Conductive Polymer. *Nano Lett.* **2015**, *15*, 6276–6281. [[CrossRef](#)]
64. Zhao, X.; Wu, H.; Guo, B.; Dong, R.; Qiu, Y.; Ma, P.X. Antibacterial anti-oxidant electroactive injectable hydrogel as self-healing wound dressing with hemostasis and adhesiveness for cutaneous wound healing. *Biomaterials* **2017**, *122*, 34–47. [[CrossRef](#)]
65. Augst, A.D.; Kong, H.J.; Mooney, D.J. Alginate Hydrogels as Biomaterials. *Macromol. Biosci.* **2006**, *6*, 623–633. [[CrossRef](#)]
66. Badawi, N.M.; Batoo, K.M. Conductive Nanocomposite Cotton Thread Strands for Wire and Industrial Applications. *J. Electron. Mater.* **2020**, *49*, 6483–6491. [[CrossRef](#)]
67. Vietri, U.; Guadagno, L.; Raimondo, M.; Vertuccio, L.; Lafdi, K. Nanofilled epoxy adhesive for structural aeronautic materials. *Compos. Part B-Eng.* **2014**, *61*, 73–83. [[CrossRef](#)]
68. Gao, Z.; Kong, L.; Jin, R.; Liu, X.; Hu, W.; Gao, G. Mechanical, adhesive and self-healing ionic liquid hydrogels for electrolytes and flexible strain sensors. *J. Mater. Chem.:C* **2020**, *8*, 11119–11127. [[CrossRef](#)]
69. Zhao, Q.; Liu, J.; Wu, Z.; Xu, X.; Ma, H.; Hou, J.; Xu, Q.; Yang, R.; Zhang, K.; Zhang, M.; et al. Robust PEDOT:PSS-based hydrogel for highly efficient interfacial solar water purification. *Chem. Eng. J.* **2022**, *442*, 136284. [[CrossRef](#)]
70. Zeng, J.; Dong, L.; Sha, W.; Wei, L.; Guo, X. Highly stretchable, compressible and arbitrarily deformable all-hydrogel soft supercapacitors. *Chem. Eng. J.* **2020**, *383*, 123098. [[CrossRef](#)]
71. Babeli, I.; Ruano, G.; Puiggali-Jou, A.; Ginebra, M.-P.; Alemán, C.; Garcia-Torres, J. Self-Healable and Eco-Friendly Hydrogels for Flexible Supercapacitors. *Adv. Sustain. Syst.* **2021**, *5*, 2000273. [[CrossRef](#)]
72. Wu, Q.; Wei, J.; Xu, B.; Liu, X.; Wang, H.; Wang, W.; Wang, Q.; Liu, W. A robust, highly stretchable supramolecular polymer conductive hydrogel with self-healability and thermo-processability. *Sci. Rep.* **2017**, *7*, 41566. [[CrossRef](#)] [[PubMed](#)]
73. Zhao, Y.; Liang, Q.; Mugo, S.M.; An, L.; Zhang, Q.; Lu, Y. Self-Healing and Shape-Editable Wearable Supercapacitors Based on Highly Stretchable Hydrogel Electrolytes. *Adv. Sci.* **2022**, *9*, 2201039. [[CrossRef](#)] [[PubMed](#)]
74. Bhat, M.A.; Rather, R.A.; Shalla, A.H. PEDOT and PEDOT:PSS conducting polymeric hydrogels: A report on their emerging applications. *Synth. Met.* **2021**, *273*, 116709. [[CrossRef](#)]
75. Zhang, Y.-F.; Guo, M.-M.; Zhang, Y.; Tang, C.Y.; Jiang, C.; Dong, Y.; Law, W.-C.; Du, F.-P. Flexible, stretchable and conductive PVA/PEDOT:PSS composite hydrogels prepared by SIPN strategy. *Polym. Test.* **2020**, *81*, 106213. [[CrossRef](#)]
76. Peng, K.; Zhang, J.; Yang, J.; Lin, L.; Gan, Q.; Yang, Z.; Chen, Y.; Feng, C. Green Conductive Hydrogel Electrolyte with Self-Healing Ability and Temperature Adaptability for Flexible Supercapacitors. *ACS Appl. Mater. Interfaces* **2022**, *14*, 39404–39419. [[CrossRef](#)]

77. Solazzo, M.; Monaghan, M.G. Structural crystallisation of crosslinked 3D PEDOT:PSS anisotropic porous biomaterials to generate highly conductive platforms for tissue engineering applications. *Biomater. Sci.* **2021**, *9*, 4317–4328. [[CrossRef](#)]
78. Li, J.; Yan, W.; Zhang, G.; Sun, R.; Ho, D. Natively stretchable micro-supercapacitors based on a PEDOT:PSS hydrogel. *J. Mater. Chem. C* **2021**, *9*, 1685–1692. [[CrossRef](#)]

**Disclaimer/Publisher’s Note:** The statements, opinions and data contained in all publications are solely those of the individual author(s) and contributor(s) and not of MDPI and/or the editor(s). MDPI and/or the editor(s) disclaim responsibility for any injury to people or property resulting from any ideas, methods, instructions or products referred to in the content.